

## Cesium carbonate as a functional interlayer for polymer photovoltaic devices

Fang-Chung Chen, Jyh-Lih Wu, Sidney S. Yang, Kuo-Huang Hsieh, and Wen-Chang Chen

Citation: [Journal of Applied Physics](#) **103**, 103721 (2008); doi: 10.1063/1.2937202

View online: <http://dx.doi.org/10.1063/1.2937202>

View Table of Contents: <http://scitation.aip.org/content/aip/journal/jap/103/10?ver=pdfcov>

Published by the [AIP Publishing](#)

---

### Articles you may be interested in

[Efficient polymer solar cells with a solution-processed gold chloride as an anode interfacial modifier](#)

Appl. Phys. Lett. **102**, 163302 (2013); 10.1063/1.4803039

[Solution processed sodium chloride interlayers for efficient electron extraction from polymer solar cells](#)

Appl. Phys. Lett. **101**, 053309 (2012); 10.1063/1.4742161

[Inverted organic solar cells comprising a solution-processed cesium fluoride interlayer](#)

Appl. Phys. Lett. **98**, 053303 (2011); 10.1063/1.3548860

[Highly efficient inverted polymer solar cell by low temperature annealing of Cs<sub>2</sub>CO<sub>3</sub> interlayer](#)

Appl. Phys. Lett. **92**, 173303 (2008); 10.1063/1.2918983

[Electronic structures and electron-injection mechanisms of cesium-carbonate-incorporated cathode structures for organic light-emitting devices](#)

Appl. Phys. Lett. **88**, 152104 (2006); 10.1063/1.2192982

---



## Re-register for Table of Content Alerts

Create a profile.



Sign up today!



# Cesium carbonate as a functional interlayer for polymer photovoltaic devices

Fang-Chung Chen,<sup>1,a)</sup> Jyh-Lih Wu,<sup>2</sup> Sidney S. Yang,<sup>2</sup> Kuo-Huang Hsieh,<sup>3</sup> and Wen-Chang Chen<sup>3</sup>

<sup>1</sup>Department of Photonics and Display Institute, National Chiao Tung University, Hsinchu, Taiwan 300, Republic of China

<sup>2</sup>Institute of Photonics Technologies, National Tsing Hua University, Hsinchu, Taiwan 300, Republic of China

<sup>3</sup>Institute of Polymer Science and Engineering, National Taiwan University, Taipei, Taiwan 106, Republic of China

(Received 31 July 2007; accepted 29 March 2008; published online 29 May 2008)

The device characteristics of polymer solar cells with cesium carbonate ( $\text{Cs}_2\text{CO}_3$ ) as an electron-injection interlayer have been investigated. It is found that the insertion of  $\text{Cs}_2\text{CO}_3$  at the cathode interface improves the device power conversion efficiency from 2.3% to 3.1%. In order to further understand the mechanism, the interfacial interaction between the active organic layer and the cathode was studied by x-ray photoemission spectroscopy (XPS). The results of XPS measurement indicate the fact that a portion of electrons transfer from the interlayer into the organic layer, resulting in *n*-type doping. The *n*-doping effect enhances the efficiency of electron injection and collection. Further, the maximum open-circuit voltage ( $V_{oc}$ ) was determined from its temperature dependence. For the device with  $\text{Cs}_2\text{CO}_3$ , the maximum  $V_{oc}$  is extremely close to the corresponding value of the energy difference between the highest occupied molecular orbital of the electron donor and the lowest unoccupied molecular orbital of the electron acceptor, suggesting a better Ohmic contact. All evidences indicated that  $\text{Cs}_2\text{CO}_3$  is a promising candidate as an interlayer to improve the device performance. © 2008 American Institute of Physics.

[DOI: [10.1063/1.2937202](https://doi.org/10.1063/1.2937202)]

## I. INTRODUCTION

Organic photovoltaic devices (OPVs) have attracted much attention due to their unique advantages, such as light weight, low-cost fabrication, and flexibility. However, the power conversion efficiency (PCE) of organic solar cells is still too low to be used for commercial applications. Therefore, many methods, such as postproduction treatment and solvent annealing, to improve the device performance have been proposed.<sup>1-5</sup> Today, most efficient OPVs are fabricated based on the bulk-heterojunction (BHJ) concept,<sup>1-7</sup> in which conjugated polymers (electron donors) and fullerenes (electron acceptors) form a three dimensional network with a large area of phase-separation interface. When photons are absorbed by the organic materials, electron-hole pairs (excitons) with strong binding energy are generated. The excitons subsequently dissociate, forming free carriers, while they diffuse to the interface between the electron donor and the acceptor. Then, these photogenerated holes and electrons transport through the donor and acceptor materials, respectively, toward the electrodes, resulting in photocurrent eventually. So far, the most efficient BHJ structure consists typically of poly(3-hexylthiophene) (P3HT) as the donor and [6,6]-phenyl C61-butyric acid methyl ester (PCBM) as the acceptor.<sup>1-7</sup> PCE of OPVs based on P3HT/PCBM BHJ structures up to 5% has been reported.<sup>1-7</sup>

One of the key issues to high-efficiency OPVs is to de-

crease the contact resistances of the anode and the cathode. For example, an ultrathin insulating interlayer, such as LiF, is commonly inserted between the organic active layer and the Al cathode to enhance the efficiency of electron collection.<sup>8,9</sup> This method has been actually commonly used to improve the electron injection in organic light-emitting diodes (OLEDs).<sup>10,11</sup> Among these insulating interlayer materials, cesium carbonate ( $\text{Cs}_2\text{CO}_3$ ) is recently reported to be one of the best electron-injection materials.<sup>12-16</sup> For example, Wu *et al.* demonstrated that  $\text{Cs}_2\text{CO}_3$  can improve the device performance of OLEDs due to the strong *n*-doping effect regardless of the cathode electrode materials from the results of ultraviolet photoemission spectroscopy (UPS) and x-ray photoemission spectroscopy (XPS).<sup>14</sup> Li *et al.* utilized the quartz crystal microbalance to estimate the possible evaporation behavior of  $\text{Cs}_2\text{CO}_3$ .<sup>15</sup> They found that  $\text{Cs}_2\text{CO}_3$  decomposed into metallic Cs and gases during thermal evaporation following



The thin Cs layer with an extremely low work function (1.9 eV) reduces the barrier height at the interface between the organics and the cathode. More recently, Huang *et al.* also indicated that thermally evaporated  $\text{Cs}_2\text{CO}_3$  decomposes into  $\text{CsO}_2$  and cesium suboxides, yielding a heavily doped *n*-type semiconductor, which exhibits a low work function.<sup>16</sup> This interfacial material tends to react with Al and create a Al-O-Cs complex, which further lowers the work function.<sup>16</sup> Further, the effect of  $\text{Cs}_2\text{CO}_3$  interfacial layer on

<sup>a)</sup>Electronic mail: fchen@mail.nctu.edu.tw.

polymer photovoltaic devices with both regular and inverted configurations has also been investigated by Li *et al.*<sup>13</sup> Because the  $\text{Cs}_2\text{CO}_3$  thin film shows a low work function, which is deduced from the UPS measurement, the authors indicated that the polymer/ $\text{Cs}_2\text{CO}_3$  contact is Ohmic.

In this work, we used P3HT as the electron donor material and PCBM as the electron acceptor to fabricate OPVs. In addition, an interlayer of  $\text{Cs}_2\text{CO}_3$  was inserted between the active layer and the cathode. With this ultrathin interlayer, the device PCE was found to improve from 2.3% to 3.1%. Furthermore, the XPS measurement indicated that the improvement could be attributed to the *n*-type doping effect on the active layer. Finally, the result of  $V_{oc}$  temperature dependence suggested that a better contact was formed at the organics/cathode interface after inserting  $\text{Cs}_2\text{CO}_3$ . A more extended study on the effect of the  $\text{Cs}_2\text{CO}_3$  interlayer on the device performance is presented.

## II. EXPERIMENT

The devices were fabricated on patterned indium tin oxide (ITO) glass substrates. The ITO substrates were cleaned in an ultrasonic bath with detergent, acetone, and isopropanol sequentially and finally were rinsed in de-ionized water. After cleaning, the ITO glass was dried in an oven and then treated with UV ozone. By spin coating, the cleaned substrates were covered with a thin layer of poly(3,4-ethylenedioxythiophene): poly(styrenesulfonate) (PEDOT:PSS) and subsequently baked at 120 °C for 60 min. The active layer of P3HT:PCBM (weight ratio=1:1) was spin coated from a 1.7 wt % solution of 1, 2-dichlorobenzene on the top of PEDOT:PSS. Before the deposition of the cathode, the active film was thermally annealed at 110 °C for 15 min. To complete the device, an interlayer of  $\text{Cs}_2\text{CO}_3$  (~1 nm) and of Al (100 nm) were thermally evaporated through a shadow mask to define the device area (0.12 cm<sup>2</sup>) under a vacuum of  $\sim 6 \times 10^{-6}$  torr. The schematic device structure was shown in Fig. 1(a). The energy level diagrams of all materials used in this study are also shown in Fig. 1(b). The current density–voltage (*J*-*V*) curves of the devices were obtained from a Keithley 2400 source-measure unit. The photocurrent was obtained under illumination from a Thermal Oriel solar simulator (AM1.5G). The interfacial interaction between the organic layer and the cathode was examined by XPS. The XPS measurement was carried out by using a monochromatic Al *K* $\alpha$  source (1486.6 eV). The absolute energy resolution was set to be about 0.1 eV. The atomic force microscopy (AFM) images were taken on DI-Veeco multi-mode AFM with a nanoscope controller.

## III. RESULTS AND DISCUSSION

Figure 2 shows the *J*-*V* curves for the devices with and without the  $\text{Cs}_2\text{CO}_3$  interlayer under the AM1.5G illumination (100 mW/cm<sup>2</sup>). Before the insertion of  $\text{Cs}_2\text{CO}_3$ , the open-circuit voltage ( $V_{oc}$ ) was 0.41 V; the short circuit current density ( $J_{sc}$ ) was 11.2 mA/cm<sup>2</sup>; the fill factor (FF) was 0.50, resulting in the PCE of 2.3%. On the other hand, after the insertion of  $\text{Cs}_2\text{CO}_3$ ,  $J_{sc}$  decreased slightly to

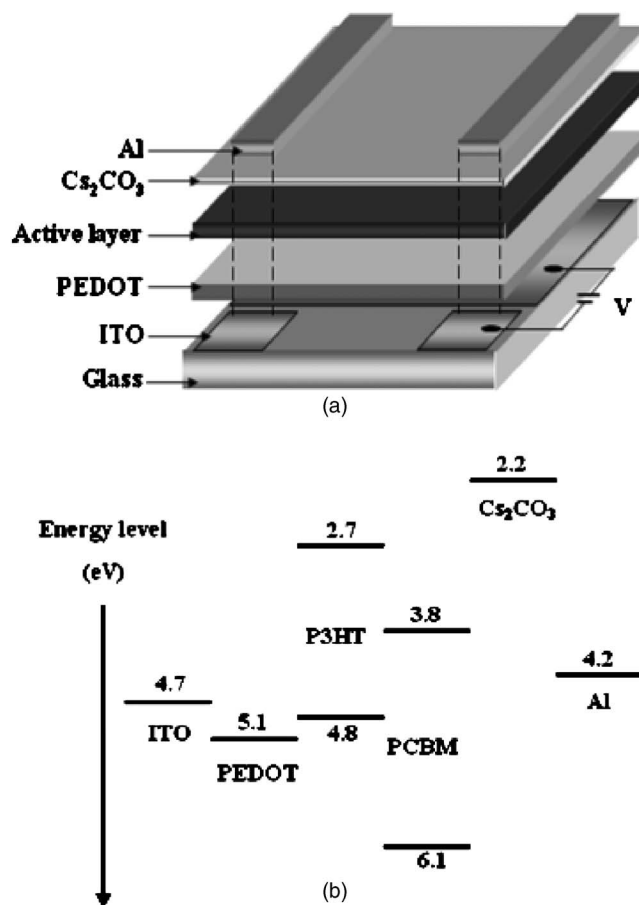


FIG. 1. (a) Schematic device structure of the polymer solar cells in this study. (b) Energy level diagram of all materials used in this study.

9.5 mA/cm<sup>2</sup>. However, the  $V_{oc}$  increased dramatically to 0.56 V, and a FF of 0.60 was achieved. The calculated PCE improved to 3.1%.

The series resistances ( $R_s$ ) of the devices were also calculated from the *J*-*V* curves in the dark. The device  $R_s$  significantly reduced from 13.0 to 3.1  $\Omega$  cm<sup>2</sup> after the incorpora-

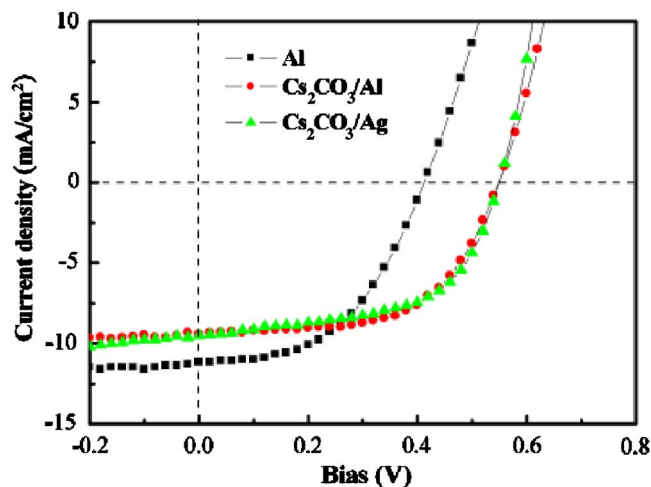


FIG. 2. (Color online) Current density (*J*)–voltage (*V*) characteristics of polymer solar cells with various cathodes under 100 mW/cm<sup>2</sup> illumination (AM1.5G). (a) Al cathode (square), (b)  $\text{Cs}_2\text{CO}_3$ /Al cathode (circle), and (c)  $\text{Cs}_2\text{CO}_3$ /Ag cathode (triangle).

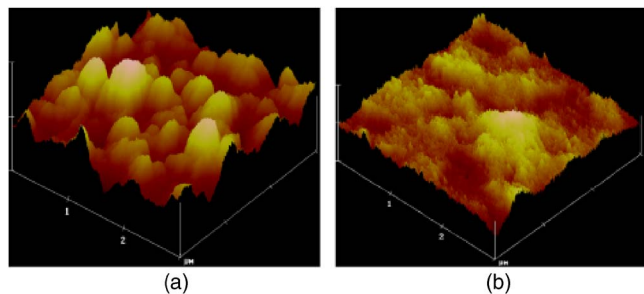


FIG. 3. (Color online) AFM images ( $3 \times 3 \mu\text{m}^2$ ) of the interfacial morphology beneath the cathode of the device (a) without  $\text{Cs}_2\text{CO}_3$  interlayer and (b) with  $\text{Cs}_2\text{CO}_3$  interlayer.

ration of  $\text{Cs}_2\text{CO}_3$ . Main contributions to the  $R_s$  include the contact resistance between the electrodes and the organics as well as the bulk resistance of the organics. Since the bulk resistance remained unchanged after the modification, the reduction in  $R_s$  should result from the improved contact at the cathode. Moreover, the larger FF of the device with  $\text{Cs}_2\text{CO}_3$  also reflects the reduction in  $R_s$ . Therefore, it is inferred that the interlayer improves the interface between the organic layer and Al. Furthermore, since the  $V_{oc}$  is closely related to the energy difference between the work functions of the cathode and the anode, the increased  $V_{oc}$  of the device with  $\text{Cs}_2\text{CO}_3$  also suggests that the work function of the cathode was reduced.<sup>13</sup> Thus, one would expect that the modification at the cathode facilitates the electron injection (collection). In short, the improved device characteristics indicate that  $\text{Cs}_2\text{CO}_3$  acts as an effective functional interlayer to enhance the device performance.

To further understand the nature of the cathode interfaces, AFM was employed to investigate the interfacial morphology. The surfaces of the polymer blends were examined after the removal of the Al thin film by stick tapes. The images presented in Fig. 3 reveal apparently different physical properties of the interfaces. From the AFM images, one can see that the surface became smoother and the root-mean-square roughness decreased from 11.9 to 7.4 nm after the insertion of  $\text{Cs}_2\text{CO}_3$ . The result indicates that the adhesion between the polymer blends and Al became weaker after the deposition of  $\text{Cs}_2\text{CO}_3$ . The insertion of  $\text{Cs}_2\text{CO}_3$  possibly decreased the wettability of Al on the polymer films. Further, because the thickness of  $\text{Cs}_2\text{CO}_3$  was only  $\sim 1$  nm, the deposition of this layer resulted in a nanoscale island structure on the polymer surface. After the deposition of Al, high density voids and/or defects eventually formed at the interface, which might reduce the physical adhesion forces between polymer blends and Al. Since the defects at the interface might act as exciton quenching sites, we speculate that the reduction in the photocurrent after the use of  $\text{Cs}_2\text{CO}_3$  (Fig. 2) is attributed to the quenching of photoinduced excitons at the polymer/metal interface.

The possible interaction at the interface between the active blend and the cathode was further investigated by XPS. The C(1s) and Cs(3d) core-level spectra are shown in Fig. 4. In Fig. 4(a), the C(1s) core-level spectrum of the pristine active layer shows a main peak at 284.6 eV, which is asso-

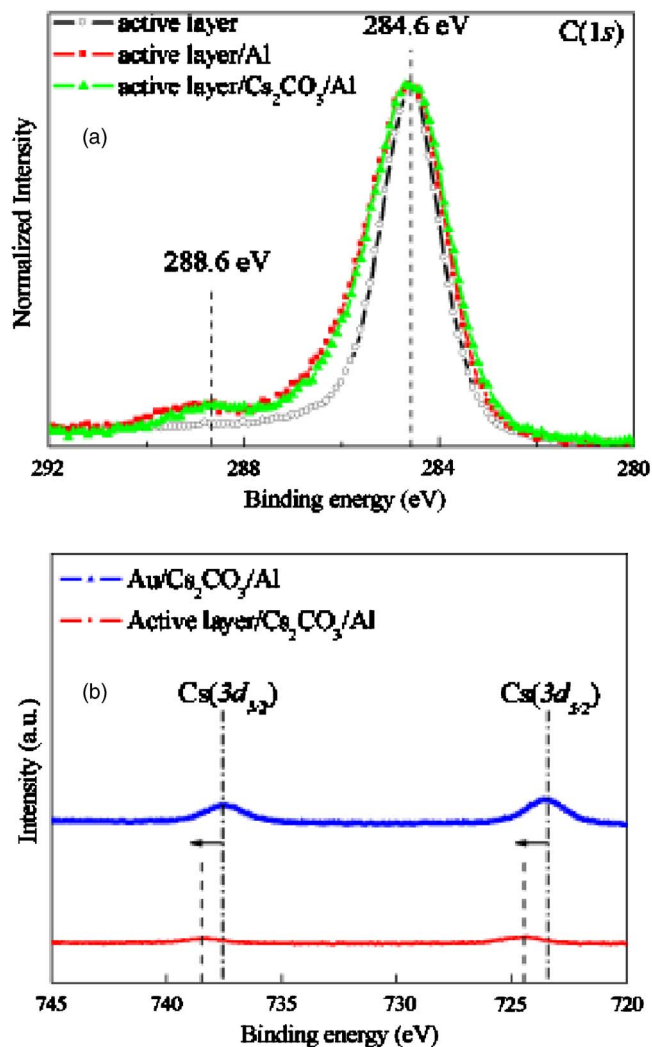


FIG. 4. (Color online) Core-level spectra of XPS measurement. (a) C(1s) for various samples: pristine active layer (circles), active layer/Al (squares), and active layer/ $\text{Cs}_2\text{CO}_3$ /Al (triangles). (b) Cs(3d) for Au/ $\text{Cs}_2\text{CO}_3$ /Al (triangles) and active layer/ $\text{Cs}_2\text{CO}_3$ /Al (squares). The thicknesses are 1 and 4 nm for  $\text{Cs}_2\text{CO}_3$  and Al, respectively.

ciated with hydrocarbon atoms (C–C and C–H).<sup>17</sup> The second C(1s) peak at 288.6 eV can be obviously observed after the deposition of Al on the top of the active layer. The characteristics in the C(1s) spectrum is attributed to the strong interaction between Al and organics.<sup>17</sup> In Fig. 4(b), the Cs(3d<sub>3/2</sub>) and Cs(3d<sub>5/2</sub>) peaks of the Au/ $\text{Cs}_2\text{CO}_3$ /Al sample locate at 737.9 and 723.9 eV, respectively, where the Au was the substrate, and  $\text{Cs}_2\text{CO}_3$  and Al were deposited sequentially. When Au was replaced by the organic active material (active organic blend/ $\text{Cs}_2\text{CO}_3$ /Al), the Cs(3d) peaks both shift to higher binding energies, indicating that electron transfers from the interlayer to the active layer.<sup>14</sup> Thus, this doping process may enhance the electron injection from the cathode into the active layer. The reduced  $R_s$  for the device with the  $\text{Cs}_2\text{CO}_3$ /Al cathode, resulting in the enhanced electron injection (collection), is therefore expected to be attributed to the *n*-doping effect induced by the reaction between  $\text{Cs}_2\text{CO}_3$  and the active blend. The XPS results are consistent with a previous mechanism proposed by Wu *et al.*<sup>14</sup> Further, when Al was replaced by Ag, the device with  $\text{Cs}_2\text{CO}_3$ /Ag as

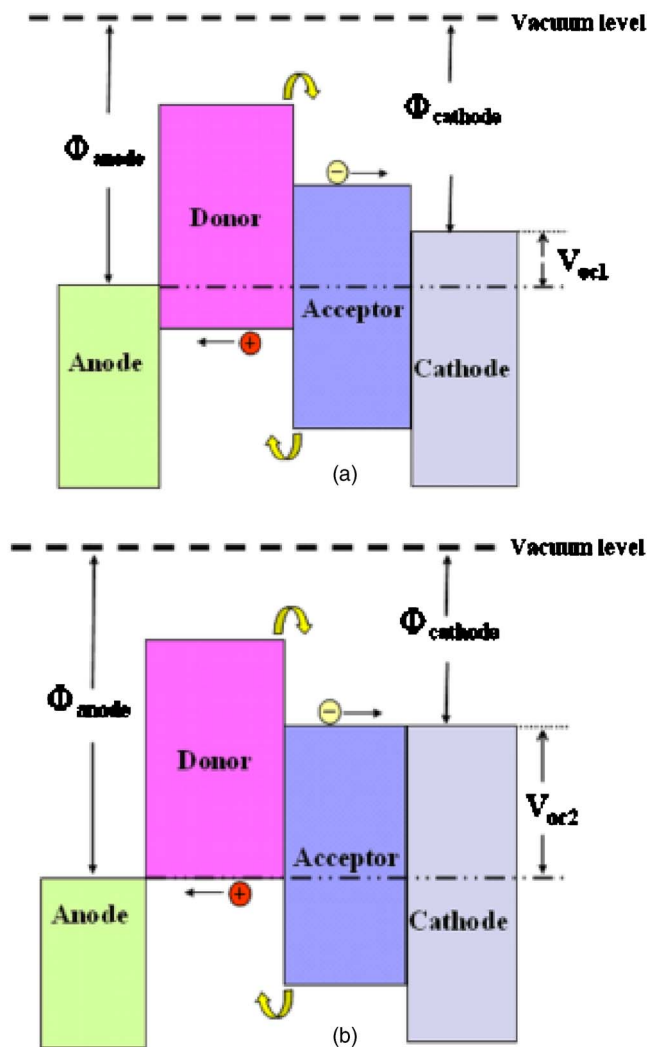


FIG. 5. (Color online) (a) Open-circuit voltage ( $V_{oc}$ ) for the organic BHJ solar cells with non-Ohmic contacts. (b) Open-circuit voltage ( $V_{oc}$ ) for the organic BHJ solar cells with Ohmic contacts.

the cathode also exhibited comparable electric characteristics ( $V_{oc}=0.55$  V,  $J_{sc}=9.52$  mA/cm<sup>2</sup>, FF=56.9, and PCE=2.98%), as shown in Fig. 2. Therefore, the superior ability of electron injection for Cs<sub>2</sub>CO<sub>3</sub> is believed to be insensitive to the cathode metal used. This is also in agreement with the results of previous reports.<sup>13–16</sup> Summarizing the above results, it can be concluded that Cs<sub>2</sub>CO<sub>3</sub> is a promising candidate as an interlayer for improving the efficiency of electron collection and enhancing the device performance of OPVs.

For organic BHJ solar cells, their maximum value of  $V_{oc}$  [ $(V_{oc})_{max}$ ] depends on the characteristics of the organic/metal contacts.<sup>18</sup> In the case of non-Ohmic contacts, as illustrated in Fig. 5(a),  $(V_{oc})_{max}$  is given by the difference of work functions between the anode and the cathode, which follows the metal-insulator-metal model. Therefore,  $(V_{oc})_{max}$  is equal to  $V_{oc1}$ . On the other hand, the maximum  $V_{oc}$  for the devices with Ohmic contacts is governed by the energy difference between the lowest unoccupied molecular orbital (LUMO) of the acceptor and the highest occupied molecular orbital (HOMO) of the donor, thus leading to  $(V_{oc})_{max}=V_{oc2}$ , as depicted in Fig. 5(b).<sup>18</sup> In general,  $V_{oc}$  can be expressed as follows:<sup>19</sup>

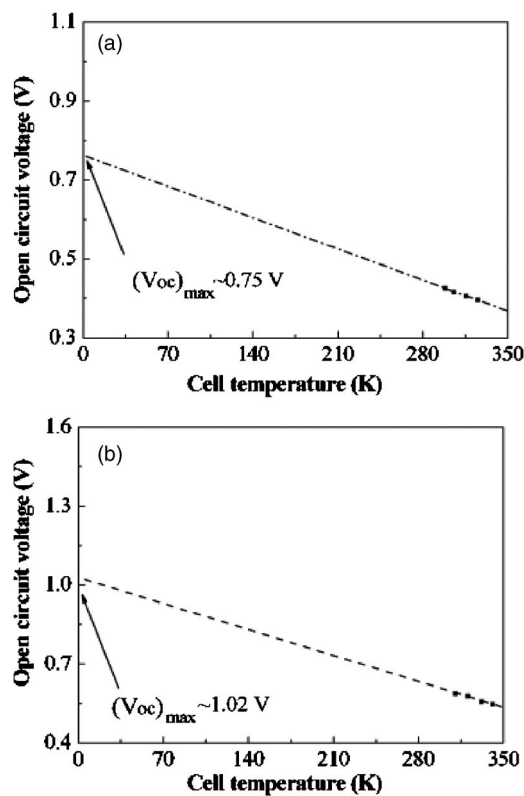


FIG. 6. Temperature dependence of  $V_{oc}$  for devices with the following structures: (a) ITO/PEDOT: PSS/P3HT: PCBM/Al and (b) ITO/PEDOT: PSS/P3HT: PCBM/Cs<sub>2</sub>CO<sub>3</sub>/Al.

$$V_{oc} = \frac{E_{gap}}{q} - \frac{kT}{q} \ln \left[ \frac{(1-P)\gamma N_c^2}{PG} \right], \quad (2)$$

where  $P$  is the dissociation possibility of a bound electron-hole pair into free charge carriers,  $G$  is the generation rate of bound electron-hole pairs,  $\gamma$  is the Langevin recombination constant, and  $N_c$  is the effective density of states. According to Eq. (2),  $(V_{oc})_{max}$  can be determined from the temperature dependence of  $V_{oc}$ ,<sup>18,20</sup> i.e., the maximum  $V_{oc}$  equals  $V_{oc}$  while the temperature is equal to 0 K. For the devices in this study, the temperature dependence of  $V_{oc}$  was shown in Fig. 6, and the extrapolation to 0 K provides the maximum values of  $V_{oc}$ , which are equal to 0.75 and 1.02 V for the devices with Al cathode and Cs<sub>2</sub>CO<sub>3</sub>/Al cathode, respectively. As a result, for the device without the interlayer, the obtained  $(V_{oc})_{max}$  (0.75 V) suggests a nonideal contact at the cathode. On the other hand, for the device with Cs<sub>2</sub>CO<sub>3</sub>, the maximum  $V_{oc}$  (1.02 V) is extremely close to the corresponding value of the energy difference between the HOMO of P3HT (4.8 eV) and the LUMO of PCBM (3.8 eV),<sup>21</sup> indicating the fact that both contacts are Ohmic. This is well consistent with the result observed by Huang *et al.*<sup>16</sup> They utilized the impedance spectroscopy to prove that an Ohmic contact can be formed at the Cs<sub>2</sub>CO<sub>3</sub> interface. Therefore, the  $V_{oc}$  temperature dependence further supports the improvement of the cathode contact by inserting an ultrathin interlayer of Cs<sub>2</sub>CO<sub>3</sub>.

#### IV. CONCLUSIONS

We have investigated the device characteristics of polymer solar cells with Cs<sub>2</sub>CO<sub>3</sub> interlayer as well as the mecha-

nism of the improved contact at the  $\text{Cs}_2\text{CO}_3/\text{Al}$  cathode. We found that the incorporation of  $\text{Cs}_2\text{CO}_3$  interlayer improves the device performance. The PCE improved from 2.3% to 3.1%. From the examination of the interfacial interaction between the active layer and the cathode, the XPS measurement revealed that a portion of electrons transfer from the interlayer into the organic layer, resulting in *n*-type doping. The *n*-doping effect on the active blend is responsible for the enhanced efficiency of electron injection and collection. In addition, we determined the maximum  $V_{\text{oc}}$  from the temperature dependence of the device  $V_{\text{oc}}$ . The result further confirms that  $\text{Cs}_2\text{CO}_3/\text{Al}$  can form a better Ohmic contact with the organic layer, and thereby reduce the device series resistance. In conclusion,  $\text{Cs}_2\text{CO}_3$  indeed acts as a promising interlayer to improve the device performance of organic solar cells.

### ACKNOWLEDGMENTS

The authors would like to thank the financial support from Ministry of Economic Affairs under Contract No. 96-EC-17-A-08-S1-015. F.-C.C. would also like to thank the support from National Science Council (NSC-95-ET-7-009-001-ET) and Ministry of Education ATU program.

<sup>1</sup>F. Padinger, R. S. Rittberger, and N. S. Sariciftci, *Adv. Funct. Mater.* **13**, 85 (2003).

<sup>2</sup>G. Li, V. Shrotriya, J. S. Huang, Y. Yao, T. Moriarty, K. Emery, and Y. Yang, *Nat. Mater.* **4**, 864 (2005).

<sup>3</sup>J. Y. Kim, S. H. Kim, H. H. Lee, K. Lee, W. Ma, X. Gong, and A. J. Heeger, *Adv. Mater. (Weinheim, Ger.)* **18**, 572 (2006).

<sup>4</sup>W. Ma, C. Yang, X. Gong, K. Lee, and A. J. Heeger, *Adv. Funct. Mater.* **15**, 1617 (2005).

<sup>5</sup>C. J. Ko, Y. K. Lin, F. C. Chen, and C. W. Chu, *Appl. Phys. Lett.* **90**, 063509 (2007).

<sup>6</sup>M. R. Reyes, K. Kim, and D. L. Carroll, *Appl. Phys. Lett.* **87**, 083506 (2005).

<sup>7</sup>K. Kim, J. Liu, M. A. G. Nambhothiry, and D. L. Carroll, *Appl. Phys. Lett.* **90**, 163511 (2007).

<sup>8</sup>C. J. Brabec, S. E. Shaheen, C. Winder, and N. S. Sariciftci, *Appl. Phys. Lett.* **80**, 1288 (2002).

<sup>9</sup>E. Ahlswede, J. Hanisch, and M. Powalla, *Appl. Phys. Lett.* **90**, 163504 (2007).

<sup>10</sup>L. S. Hung, C. W. Tang, and M. G. Mason, *Appl. Phys. Lett.* **70**, 152 (1997).

<sup>11</sup>Y. Yuan, D. Grozea, S. Han, and Z. H. Lu, *Appl. Phys. Lett.* **85**, 4959 (2004).

<sup>12</sup>J. Huang, G. Li, E. Wu, Q. Xu, and Y. Yang, *Adv. Mater. (Weinheim, Ger.)* **18**, 114 (2006).

<sup>13</sup>G. Li, C. W. Chu, V. Shrotriya, J. Huang, and Y. Yang, *Appl. Phys. Lett.* **88**, 253503 (2006).

<sup>14</sup>C. I. Wu, C. T. Lin, Y. H. Chen, M. H. Chen, Y. J. Lu, and C. C. Wu, *Appl. Phys. Lett.* **88**, 152104 (2005).

<sup>15</sup>Y. Li, D. Q. Zhang, L. Duan, R. Zhang, L. D. Wang, and Y. Qiu, *Appl. Phys. Lett.* **90**, 012119 (2007).

<sup>16</sup>J. Huang, Z. Xu, and Y. Yang, *Adv. Funct. Mater.* **17**, 1966 (2007).

<sup>17</sup>T. F. Guo, F. S. Yang, Z. J. Tsai, T. C. Wen, S. N. Hsieh, Y. S. Fu, and C. T. Chung, *Appl. Phys. Lett.* **88**, 113501 (2006).

<sup>18</sup>V. D. Mihailetchi, P. W. M. Blom, J. C. Hummelen, and M. T. Rispen, *J. Appl. Phys.* **94**, 6849 (2003).

<sup>19</sup>L. J. A. Koster, V. D. Mihailetchi, R. Ramaker, and P. W. M. Blom, *Appl. Phys. Lett.* **86**, 123509 (2005).

<sup>20</sup>E. A. Katz, D. Faiman, S. M. Tuladhar, J. M. Kroon, M. M. Wienk, T. Fromherz, F. Padinger, C. J. Brabec, and N. S. Sariciftci, *J. Appl. Phys.* **90**, 5343 (2001).

<sup>21</sup>L. J. A. Koster, V. D. Mihailetchi, and P. W. M. Blom, *Appl. Phys. Lett.* **88**, 093511 (2006).